RF DESIGN OF MOBILE PHONES BY TCAD: SUITABILITY AND LIMITATIONS OF FDTD

N. Chavannes[1], R. Tay[2], N. Nikoloski[3], N. Kuster[3]

(1) ***Schmid & Partner Engineering AG (SPEAG), 8004 Zurich, (Switzerland)***
Tel. +41 1 632 2755, Fax +41 1 632 1057, E-mail chavanne@speag.com
(2) *Motorola Electronics Private Limited, Singapore*
(3) *Foundation for Research on Information Technologies in Society (IT'IS), Switzerland*

ABSTRACT

This study discusses the general suitability and possible limitations of an enhanced Finite-Difference Time-Domain (FDTD) simulation environment for straightforward and efficient RF design of complex transmitters. The study was conducted using one of the latest commercial multi-band mobile phones. In the simulation different parameters were evaluated such as impedance, efficiency, far-field, as well as EM near-field distributions and the SAR. The results are compared to measurements obtained with the latest tools available. In addition, mechanical design issues which show a significant influence on the EM field behavior could be predicted by simulations and were experimentally reproduced. The obtained accurate prognosis of all essential performance parameters by straightforward simulations suggests that state-of-the-art software packages incorporating an excellent and flexible GUI as well as enhanced modeling capabilities are suitable for device design in industrial R&D environments with hardly any limitations.

INTRODUCTION

The trend to mobility and miniaturization in communication, computing and medicine is clearly heading toward a fusion of these subsystems in *pervasive computing* - interconnected intelligent subsystems providing numerous services embedded within human surrounding environments. Additional increasing consumer demand for attractive performance/price ratios as well as international mandatory safety guidelines addressing radio-frequency (RF) related possible health effects confront engineers with the development of highly efficient devices.

Technical computer aided design (TCAD) tools enable RF engineers to perform analysis and optimization of real-world designs in a straightforward user-friendly manner. However, certain requirements such as an easy import and manipulation of standard mechanical CAD data formats as well as the efficient and accurate generation of solid models and its composition are obvious. Furthermore, the tools must allow to model resolutions of a few μm embedded within relatively large environments (m) and the handling of highly non-homogeneous setups. All relevant antenna parameters must be extractable and directly comparable to measurements within the result visualization and postprocessing.

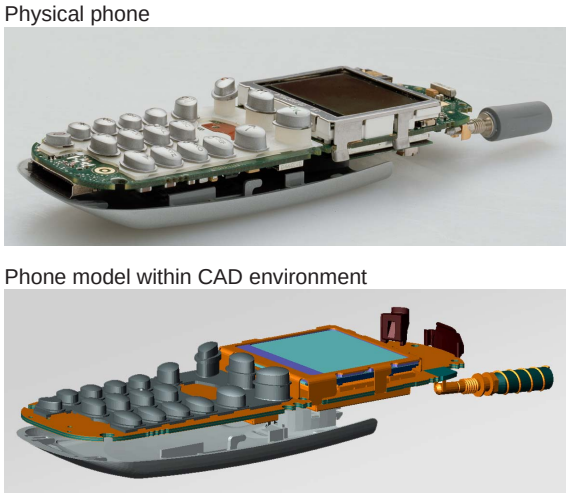

Figure 1: Motorola T250 phone: physical model (top) and its FDTD equivalent (bottom).

Figure 2: Dosimetric assessment system DASY4: free space measurement of mobile phone.

The relatively crude FDTD technique has gained growing interest because of its robustness and suitability to handle complex inhomogeneous problems. Although various enhancements of the scheme [1] have made it the most popular simulation technique, severe limitations of the method complicate its unlimited application to real-world problems which may have dimensions of only a few μm embedded within computational spaces of one meter or more. Only the latest progress in a combination of graded meshes with subgrids can enable FDTD to handle such details, such as proposed in [2]. Previous studies on mobile transmitters required strong simplifications such as rectangular PEC boxes equipped with crudely modeled antennas or have approximated the entire internal structure of CAD derived mobile phones by single PEC blocks [3], instead of including significant internal structures.

The objective of this study was to evaluate whether FDTD based tools can be utilized for supporting RF engineers in the design of mobile phones. This clearly demands that not only the outer shape of the device is simulated but all embedded electromechanical components which are RF relevant (Figure 1) and require resolutions down to 100 μm or less.

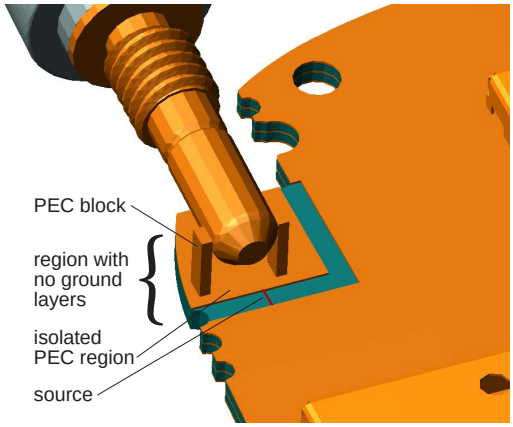

Figure 3: Excitation of the antenna - PCB structure in the modified source region.

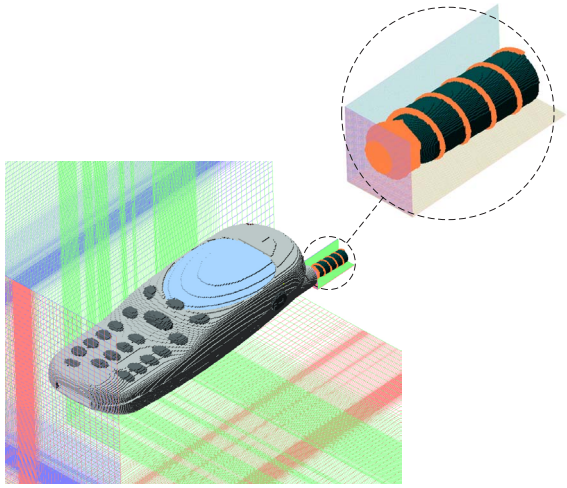

Figure 4: Application of FDTD grid: combination of graded mesh and subgrid.

METHODS: FDTD SIMULATION AND MEASUREMENT

The phone selected for this study was one of the latest commercially available tri-band phones, namely the T250 of Motorola Inc. For the purpose of this study, two samples of the phone were purchased, one was used only for measurements; the second was disassembled and optically examined. The CAD dataset was consequently exported in STL format for the purpose of modification and modeling within the FDTD based platform SEMCAD which was used for all performed simulations (*www.semcad.com*). SEMCAD is the internal EM 3-D full wave simulation platform applied within our research group for research in EM computations which has also been commercialized by Schmid & Partner Engineering AG (SPEAG), Switzerland. The solid modeling environment is based on the ACIS® modeling toolkit and allows the generation of complex 3-D objects as well as the import of whole CAD datasets. In addition, the combined platforms SEMCAD and DASY4 allowed a direct comparison of numerical and experimental data.

Special attention was drawn to the modeling of particular pieces which significantly influence the EM field behavior such as the multi-band antenna (0.65 mm wire diameter) and the PCB structure represented by five layers (2 dielectric, 3 PEC grounds) with a thickness of 450 μm and 110 μm, respectively (Figure 3) and interconnected grounds. In order to achieve a proper excitation of the mobile phone structure, a resistive (50 Ω) source was modeled which corresponds to the excitation of the physical phone by isolating the antenna from the PCB part (Figure 3). In order to reduce memory and runtime requirements, the local refinement scheme [2] is applied in combination with non-homogeneous mesh to resolve certain regions of the phone model with a high resolution. A spatial resolution of $0.2\times0.2\times0.1\,\text{mm}^3$ was chosen within the subgrid (1:2 refinement) surrounding the antenna, consisting of about 500×10^3 mesh cells in total (Figure 4). In the main grid, a non-homogeneous mesh using an increasing mesh step from 0.2 mm up to 7 mm (grading ratio = 1.5) was chosen, which leads to 4 million cells. The simulations including head models consisted of the same minimum and maximum mesh steps, whereby the human ear region was modeled with a $0.4\times0.4\times0.2\,\text{mm}^3$ grid resolution, leading to a total number of about 6 million cells. All simulations were bounded by a PML absorbing boundary condition (8 layers).

The measurements were conducted with the near-field scanning system DASY4 (SPEAG, Switzerland), which is the forth generation of the system described in [4] as shown in Figure 2. The scanner was equipped with the latest probes providing the required isotropy, sensitivity and spatial resolution.

RESULTS AND VALIDATION

For both GSM900 and DCS1800 systems, the middle traffic channels were utilized by radio communication tester, i.e., operations at f=902.4 MHz and f=1747.4 MHz, respectively. The phone design does not enable to directly measure the antenna input power with sufficient precision. For the purpose of this comparison, the antenna input power was determined indirectly by matching the simulated H-field distributions with measured ones from the DASY4 system. The obtained values for the antenna input power to which all reported simulation results were normalized, are 30.6 dBm (GSM900) and 29.1 dBm (DCS1800). Prior to the simulation of the complete phone model, the multiband antenna was examined by measurement and simulation as a monopole over a finite ground plane, in order to ensure proper representation of the antenna structure. In order to reduce the computational requirements, the CAD antenna structure was modeled by application of a 1:8 subgridded region around it (125 μm^3 resolution). An excellent agreement of both real and imaginary parts was obtained. The resonance frequencies in particular match very well, leading to 948 MHz and 960 MHz (lower resonance) and to 1.695 GHz and 1.712 GHz (higher resonance) for measured and simulated impedances, respectively.

Free Space: EM Near- and Far-Field Characterization

Figure 5 depicts the measured and simulated E- and H-field distributions at the DCS1800 frequency. The fields were recorded in a plane located at 10 mm above the highest point of the phone (display). The comparison of the simulated to the measured distribution shows slight deviations in the region of the maxima, mainly close to the antenna. However, the general agreement for both characteristic E- and H-field patterns is very good.

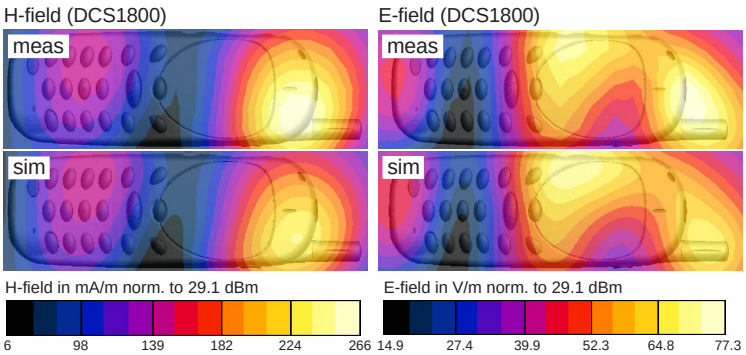

Figure 5: Simulation and measurement of E- and H-field shown in a plane at 10 mm above the phone (fields normalized to 29.1 dBm).

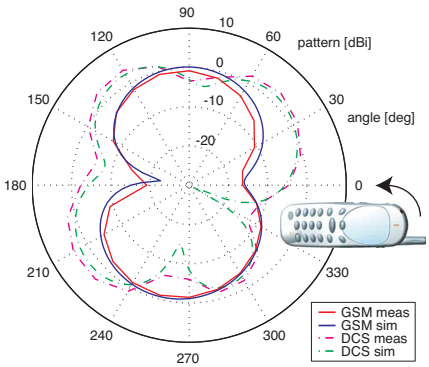

Figure 6: Meas. and sim. radiation pattern (xy plane, horiz. polarization).

The experimental assessment of the radiation characteristics has been performed in a rectangular anechoic chamber. Figure 6 shows the measured and simulated radiation pattern for horizontal polarization within the xy plane in dBi for both bands (vertical pol. in xz plane was computed but is not depicted). Good to excellent agreement between measurement and simulation is obtained for both polarizations in the planes observed.

Design Capabilities: Effect of the LCD Holder Connection

To assess the capabilities of the proposed simulation techniques with respect to design purposes, special attention was given to electromechanical parts which appeared to have a significant impact on the EM field behavior. Furthermore, the influence of FDTD grid resolution on the current distribution should be examined. Particularly in the region of the LCD which is mechanically fixed to the PCB via holder and electrically connected via 4 clamps (Figure 7), major differences between simulation and measurements were obtained initially. A closer investigation of the physical holder revealed that the clamps actually do not create a proper RF short circuit to the PCB ground. Therefore both models (CAD, physical) have been modified in a way to represent a *holder connected* and *holder floating* situation (3rd physical phone used). As shown in Figure 8, the LCD holder connection related EM field distribution predicted by the FDTD simulation is reproduced within the measured data. The characteristic near-field patterns, i.e., centralized and split current distributions on the LCD holder for the floating and short circuit connections, respectively, are obtained in both approaches.

Performance at the SAM Head

As performed in compliance testing of mobile phones, the device was placed beside the Specific Anthropomorphic Mannequin (SAM), the standard phantom IEEE and CENELEC have agreed on. Figure 9 depicts the measurement setup with the phone positioned at the SAM head as well as its corresponding CAD model within the SEMCAD platform. SAR distributions and averaged spatial peak SAR were assessed and compared for the *touch* and *15° tilted* standard test positions. Illustration 10 depicts the measured and simulated

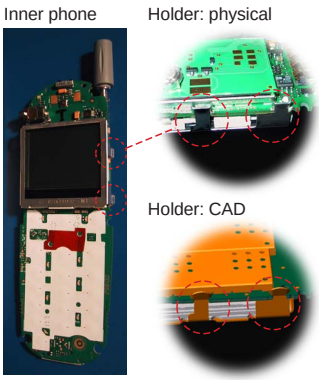

Figure 7: Metallic LCD holder: physical and CAD model.

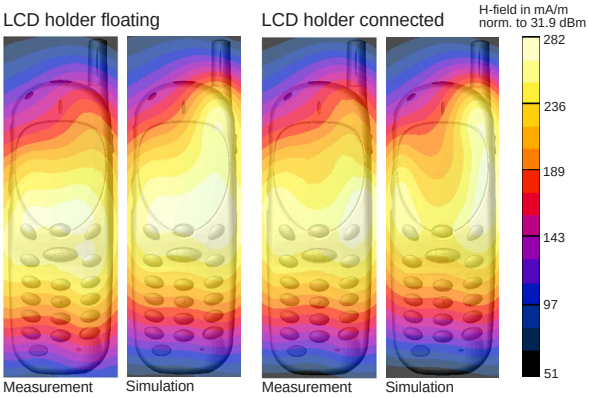

Figure 8: LCD holder: simulation and measurement in a plane at 5 mm above the phone (fields normalized to 31.9 dBm).

SAR distributions in the SAM phantom at a distance of 4.7 mm normal to the inner shape of the shell (f = 1747 MHz, log scaled). Good agreement is obtained between the measured and simulated distributions in the whole observation area. The 1 g averaged peak SAR in *touch* and *15° tilted* position at both frequencies lead to a good to excellent agreement with maximum errors $< 10\,\%$ between the experimental and numerical data for all configurations. The highest 1 g averaged SAR value was obtained for the left side *tilted* position at f=1747 MHz: meas=1.10 mW/g, sim=1.12 mW/g leading to a small difference of 1.8 %.

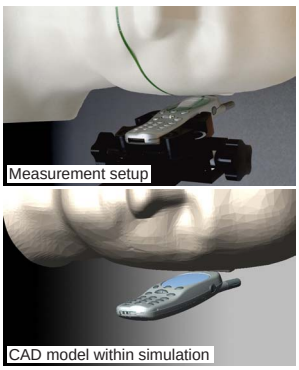

Figure 9: Phone - SAM: measurement and simulation.

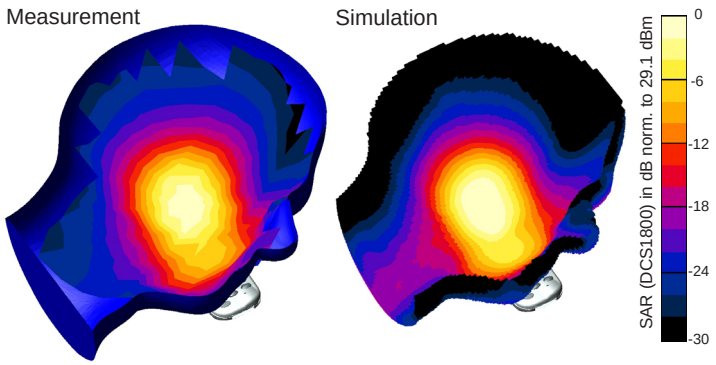

Figure 10: Measured and simulated SAR distribution within the SAM phantom (left side *touch* position, GSM1800).

CONCLUSIONS

This study demonstrates that FDTD is a suitable technique for supporting engineers in the analysis, design and optimization of transmitters, even for the most complex cases such as mobile phones operating in the vicinity of the human body. The study also clearly revealed that efficient and flexible user-interfaces as well as graded meshes combined with robust subgrids are required in order to achieve the needed resolutions of small details in the range of 100 μm within locally restricted areas of the computational domain extended by one meter or more.

REFERENCES

[1] A. Taflove, *Computational Electrodynamics - The Finite Difference Time Domain Method*, Artech House, Norwood, MA, 1995.

[2] N. Chavannes et al., "Advances in FDTD modeling capabilities for enhanced analysis of antennas embedded in complex environments", in *2001 Proceedings of the ICEAA*, Torino, Italy, Sept. 2001, pp. 353–356.

[3] A.D. Tinniswood et al., "Computations of SAR distributions for two anatomically based models of the human head using CAD files of commercial telephones and the parallelized fdtd code", *IEEE Trans on Antennas and Propagation*, vol. 46, no. 6, pp. 829–833, June 1998.

[4] T. Schmid, O. Egger, and N. Kuster, "Automated e-field scanning system for dosimetric assessments", *IEEE Transactions on Microwave Theory and Techniques*, vol. 44, pp. 105–113, Jan. 1996.